

UNLIMITED

UNCLASSIFIED

(2)

THIS IS A COPY



RSRE
MEMORANDUM No. 4269

ROYAL SIGNALS & RADAR ESTABLISHMENT

AD-A214 831

OPTICAL PROPERTIES OF ZINC SELENIDE GROWN USING
MOLECULAR BEAM DEPOSITION TECHNIQUES

Author: K Welford

DTIC
ELECTE
DEC 05 1989
S D D

PROCUREMENT EXECUTIVE,
MINISTRY OF DEFENCE,
RSRE MALVERN,
WORCS.

DISTRIBUTION STATEMENT A
Approved for public release
Distribution Unlimited

RSRE MEMORANDUM No. 4269

89 12 04 205

UNLIMITED

0054214

CONDITIONS OF RELEASE

BR-111748

.....

U

COPYRIGHT (c)
1988
CONTROLLER
HMSO LONDON

.....

Y

Reports quoted are not necessarily available to members of the public or to commercial organisations.

ROYAL SIGNALS AND RADAR ESTABLISHMENT

Memorandum 4269

TITLE: OPTICAL PROPERTIES OF ZINC SELENIDE GROWN USING MOLECULAR BEAM DEPOSITION TECHNIQUES

AUTHOR: K WELFORD

DATE: JUNE 1989

Accession For	
NTIS CRA&I	<input checked="" type="checkbox"/>
DTIC TAB	<input type="checkbox"/>
Unannounced	<input type="checkbox"/>
Justification	
By	
Distribution	
Availability Codes	
Dist	Availability
A-1	

SUMMARY

For the first time the refractive index of MBE grown ZnSe films has been measured for three different growth temperatures and the wavelength and temperature dispersions quantified. Permanent absorption, but not refractive index, changes have been identified for the first time. Possible origins of the changes are conjectured along with the significant effects they will cause in optically bistable devices. Future studies are outlined which it is hoped will go some way towards producing better quality material and thus devices.



This memorandum is for advance information. It is not necessarily to be regarded as a final or official statement by Procurement Executive, Ministry of Defence

Copyright
C
Controller HMSO London
1989

INTRODUCTION

Many optical applications are currently being found for II-VI semiconductors such as Zinc Selenide (ZnSe). Applications, like anti-reflection coatings, optical limiters [4], or as part of more complicated structures for use as optically non-linear switches with potential use in optical signal processing and optical computing [2-6] cover just a selection of uses. Up until recently thin film ZnSe used in these applications was deposited using conventional thermal evaporation techniques. Such methods were shown to lead to poor quality films. Voids within the film structure were able to take up and release water resulting in highly variable optical properties and low mechanical stability. Variations in the stoichiometry of the films provided high defect densities. Potential uses of ZnSe were dramatically hindered by these material shortcomings. Realisation that applying molecular beam epitaxy deposition techniques to the fabrication of these semiconducting thin films came from Lewis and co-workers at RSRE in the early 1980's [7]. Because most often, for the applications mentioned so far, the substrate is glass, epitaxial growth of the ZnSe film does not occur, rather a controlled polycrystalline microstructure. We therefore refer to the growth method as Molecular Beam Deposition (MBD). Realise, however, that MBE and MBD use essentially the same methods and equipment but different substrate materials. Although much improved films are now available which are fully dense, polycrystalline, and mechanically stable ie microns of deposited material can now be grown without the layer fracturing and delaminating from the substrate [8], there are still some shortcomings in the materials for critical applications. Of interest in this work are possible small refractive index and/or absorption variations which can occur under laser illumination. Such variations will have detrimental effects in any device application incorporating ZnSe layers but the area which has been first to show up these material shortcomings has been in Optical Bistability, see for example [2] and [9]. Crucial to the nonlinear properties of ZnSe is its thermal non-linearity. Temperature increases, due to absorbed laser light, induces a wavelength shift in the absorption edge which in turn causes refractive index changes. Resulting wavelength shifts in the interference maxima cause bistable operation under appropriate circumstances. Basic measurements of refractive index over the visible wavelength spectrum for a range of temperatures and for several samples grown differently in the MBD machine are studied here. With this information accurate values for $n(\lambda)$ and $dn(\lambda)/dT$ have been measured and related to growth conditions. This represents the first study of MBD grown ZnSe thin films. Previous studies on ZnSe chemical vapour deposited films at 3.8 μm and 10.6 μm wavelength over a temperature range of 80-300K have been performed by Thompson et al [10] in 1979. On bulk polycrystalline samples, using the method of minimum angle of deviation, Wunderlich and DeShazer [11] recorded the refractive index in the visible at room temperature. In addition this present study has investigated permanent alteration to the absorption edge caused by the increased temperature of the samples. As far as is known this is the first observation of such an effect in MBD grown ZnSe films, although effects of interest in CVD grown ZnSe have been studied previously [12].

Besides providing accurate values for the basic optical properties of these films, which are essential for predicting the behaviour of any device, instabilities in the optical properties of the material will be highlighted, the reasons for the instabilities conjectured, and the implications for optically bistable devices. Future work to reduce these problems will be outlined.

EXPERIMENTAL

All of the samples studied were grown using a standard MBE machine with insitu diagnostics. The ZnSe material used for growing the samples is highly pure polycrystalline ZnSe prepared by CVD from Zn vapour and hydrogen selenide and is evaporated from graphite crucibles. Out gassing of the chambers is achieved by a 180°C baking. During growth the background pressure is 10^{-8} mbar and the ZnSe is grown at a rate of $\sim 0.7 \mu\text{m/h}$, which is achieved with a crucible temperature of $\sim 780^\circ\text{C}$. Further details can be found from Lewis et al [13]. Three samples were grown on glass substrates, which were not especially prepared to be optically flat, all of nominally $5 \mu\text{m}$ thickness but at different substrate growth temperatures. The three growth temperatures were 25°C , 150°C and 300°C . Since each of these films forms a parallel sided layer their spectral response consists of a series of interference transmission maxima and minima. Some 44 maxima are observed in these films before the absorption edge at $\sim 500 \text{ nm}$ reduces the transmission to zero. From elementary theory of Fabry-Perot etalons the refractive index at a transmission maximum can be found provided the wavelength at maximum transmission is recorded, the film thickness is known and the order number, m , of the fringe is known using:

$$n = \frac{m\lambda}{2d} \quad (1)$$

A typical spectrum, recorded using a Perkin-Elmer spectrometer, is shown in Figure 1, with the order number of the transmission maxima. Determining the order numbers was achieved by recording the spectrum from 450 nm to $50 \mu\text{m}$ and establishing the $m = 1$ order from an approximate knowledge of both d and n . An accurate value for the film thickness, d , can be found by cutting the samples and taking SEM micrographs of the edge. Measurement of micrographs, such as that shown in Figure 2, leads to the following film thickness;

25°C grown sample $(4.78 \pm 0.02) \mu\text{m}$

150°C grown sample $(4.91 \pm 0.02) \mu\text{m}$

300°C grown sample $(4.71 \pm 0.02) \mu\text{m}$

An advantage of determining the refractive index using this method is that a wide wavelength range can be investigated although the film thickness does need accurate measurement. A restriction found using the minimum angle of deviation in bulk polycrystalline ZnSe by Wunderlich and DeShazer [11] was that n could not be recorded at wavelengths longer than 632.8 nm which led them to some misleading conclusions as we shall see later. Measurement of the refractive index was carried out over the restricted wavelength range of 450 nm to 800 nm. Lower wavelength cut off is dictated by the absorption in the ZnSe. Although interference maxima can be seen down the absorption edge they have only been recorded in practice down to 550 nm due to possible complicating effects resulting from the rapid change in absorption in this region. Refractive index information can be found using equation (1) even when the absorption in the film is significant. All that happens is the value of the maximum transmission, T_{max} , is reduced. Provided that the absorption does not change much over the width of the interference maxima n can be found from equation (1). Beyond 550 nm absorption is varying rapidly and this will cause T_{max} to vary significantly over the width of the interference fringe resulting in a distorted fringe shape and the maximum transmission moving toward a wavelength with lower absorption. This distortion invalidates equation (1). A schematic representation of this situation is shown in Figure 3.

Each sample was heated from 25°C to 225°C, in 50°C steps, and then cooled in the same way, recording the transmission spectrum, and hence the refractive index dispersion, at each temperature. This process was repeated a second time thus resulting in essentially four spectra at each temperature, two during heating and two during cooling phases.

RESULTS

I. Refraction

Constant temperature dispersion of bulk polycrystalline ZnSe has been investigated previously by Wunderlich and DeShazer [11] over the reduced wavelength range of 632.8 nm to 476.5 nm. In that work it was suggested that the refractive index dispersion could be adequately modelled using a two parameter, single effective oscillator, Sellmeier equation of the form

$$n^2 = 1 + \frac{A \lambda^2}{\lambda^2 - B} \quad (2)$$

Such an equation inherently assumes absorption to be zero - which is not strictly correct. A rearrangement of equation (2) leads to a linear form of the equation which affords an easy check to see if the experimental data fits the theory prediction. Expressed linearly equation (2) becomes;

$$(n^2-1)^{-1} = A^{-1} - (B/A) \lambda^{-2} \quad (3)$$

Taking a typical set of experimental data, say the 300°C grown sample at room temperature, we see in Figure 4(a) that a fit to this simple equation does not occur. For completeness the same theory and data are represented in a more usual $n \cdot v \lambda$ format in Figure 4(b). Again it is clear that a fit does not occur. Least squares fitting, using either equation (2) or (3), resulted in the following fitting parameters;

$$\begin{aligned} A &= 4.185 \pm 0.002 \\ B &= (0.0535 \pm 0.0002) \mu\text{m}^2 \end{aligned}$$

which are in only approximate agreement with Wunderlich and DeShazer who found that;

$$\begin{aligned} A &= 4.7032 \\ B &= 0.07034 \mu\text{m}^2 \end{aligned}$$

Of more importance, however, is that they concluded that Sellmeier equation did provide a fit to the experimental data with nonlinearity only setting in towards the shorter wavelengths. From figure 4(a) it is clear that nonlinearity also occurs at longer wavelengths. This fact was missed by Wunderlich and DeShazer due to the reduced wavelength range that they studied. In general Sellmeiers equation can be written as a combination of i effective oscillators, with $2i$ fitting parameters;

$$n^2 - 1 = \sum_{j=1}^i \frac{A_j \lambda^2}{\lambda^2 - B_j}$$

Extending the single oscillator model to a double oscillator model a more complicated equation results with four possible fitting parameters. In all of the nonlinear least squares fitting to each data set it was found that $B_1 = 0$, thus reducing the fitting procedure to just three parameters in an equation of the form;

$$n^2 - 1 = A_1 + \frac{A_2 \lambda^2}{\lambda^2 - B_2} \quad (4)$$

An illustration of how well equation (4) fits at each temperature for the 300°C grown sample is given in figure 5. Using equation (4) each set of experimental data, for all 3 samples at all 5 temperatures for each of the increasing and decreasing temperature phases, was least squares fitted and the fitting parameters noted. These parameters are presented in Table I, and plotted for clarity in figure 6 are the fitting coefficients for the 25°C grown sample. Figure 6 represents the data showing the most scatter. As can be appreciated from Table I and figure 6 there is no systematic variation of the coefficients between the increasing and decreasing phase, only a systematic variation of each coefficient with temperature. This is true for each of the three samples. What we have then is four sets of data at each temperature that can be averaged and then fitted to provide more accurate values for A_1 , A_2 and B_2 . Permanent refractive index changes due to heating and cooling cannot be detected with the accuracy of this experiment ($\Delta n \sim \pm 0.002$). Averaged data fitting parameters are given in Table II and plotted for clarity in figure 7. Since the variation of each of the fitting coefficients is linear the dispersion of each of the samples can now be written to include the temperature variation explicitly. The final form of the coefficients are written as;

25°C Grown Sample

$$\begin{aligned}A_1 &= 4.157 + (0.644 \times 10^{-3}) \times (T-25) \\A_2 &= 0.797 - (0.183 \times 10^{-3}) \times (T-25) \\B_2 &= 0.152 + (0.606 \times 10^{-4}) \times (T-25) \mu\text{m}^2\end{aligned}$$

150°C Grown Sample

$$\begin{aligned}A_1 &= 3.692 + (0.892 \times 10^{-3}) \times (T-25) \\A_2 &= 0.784 - (0.455 \times 10^{-3}) \times (T-25) \\B_2 &= 0.147 + (0.880 \times 10^{-4}) \times (T-25) \mu\text{m}^2\end{aligned}$$

300°C Grown Sample

$$\begin{aligned}A_1 &= 3.667 + (0.421 \times 10^{-3}) \times (T-25) \\A_2 &= 0.700 - (0.535 \times 10^{-4}) \times (T-25) \\B_2 &= 0.152 + (0.506 \times 10^{-4}) \times (T-25) \mu\text{m}^2\end{aligned}$$

Only a very broad trend is evident from these coefficients. Besides the refractive index being less for the higher growth temperature the dispersion with temperature is also less for the higher growth temperature. With these parameters it is possible to predict the refractive index at any wavelength or temperature, for a given sample, with an accuracy of ± 0.002 . Although this is not quite as good as that achieved in any of the original independent 3 parameter fits (± 0.0001) the generalised dispersion relation including temperature is seen to be more useful.

The major difference between the three samples are the refractive index values and not so much the dispersion. This fact can be appreciated by observing the dispersion curves for each of the samples measured at room temperature, see figure 8. Notice that the refractive index of the MBD layers is lower than bulk ZnSe. Using these dispersion equations the value of dn/dT as a function of wavelength can be calculated, see figure 9. This is an important parameter whenever ZnSe is used in an application where its thermal nonlinearity is utilized - such as in an optically bistable switch.

It is known from previous work on ZnSe grown on GaAs [13] that the material begins growing as an amorphous layer up to a thickness of $\sim 60\text{\AA}$ before an unstable region of $\sim 1500\text{\AA}$ where columnar crystallite growth begins to occur. Above these thicknesses highly orientated columnar growth occurs where the preferred structure is cubic with the $\langle 111 \rangle$ planes parallel to the surface. At low growth temperatures the grain structure is well formed with a typical grain column size of $\sim 250\text{\AA}$ in diameter whereas at higher growth temperatures the grains become larger, $\sim 1000\text{\AA}$, but less well defined with stacking faults extending from grain to grain. All films grown using the MBD methods have been found to be fully dense. Although the material used here is not grown on GaAs, and has not yet been fully investigated, it seems likely that the growth structure will be very similar on glass as it is on GaAs because of the amorphous layer of ZnSe which builds first.

Correlation of material differences with refractive index differences is a worthwhile study yet to be completed. Tentatively it would appear that increased defect density may be contributing to a reduction in refractive index.

II. Absorption

We have previously concentrated on the way in which the refractive index of ZnSe varies from sample to sample, and with temperature, by monitoring the effect of interference fringes. Although no discernable permanent alteration of refractive index is found due to temperature cycling the changes in absorption are most notable, especially close to the absorption edge.

Consider the 25°C grown sample the wavelength range from 450-800 nm. Initially the absorption edge is very spread out in wavelength, unlike bulk polycrystalline material which has a much sharper change in absorption corresponding to a better defined band gap, see reference [1] their figure 6. At longer wavelengths the absorption becomes more constant but still quite large as indicated by the relatively low value for T_{\max} . Heating this sample to 75°C and cooling to room temperature produces quite a different absorption response, see figure 10. Firstly notice that the refractive index has not altered significantly. However, the absorption has altered by a significant amount, not only at longer wavelengths, where T_{\max} increases from 70% to 79%, but most noticeably in the absorption edge region where the edge has become much more abrupt. If the sample is taken up to 225°C and cooled once more to room temperature we see, in figure 10, that a further, smaller, change in T_{\max} has occurred at longer wavelengths from 79% to 82%, but a more dramatic change has occurred again close to the absorption edge.

Repeating the temperature increase to 225°C and cooling to room temperature produces only slight further alterations. By far the majority of the permanent changes occur in the first heating of the material. Notice that large changes in transmission occur for small changes in temperature, just 50°C temperature increase, and that material changes are proportional to temperature change with minor further changes each time this temperature is reached. This has important implications for the stability of the material. This issue will be returned to later.

Another effect worthy of note is the way in which T_{\max} varies with temperature for a given fringe. If the value of T_{\max} is recorded for a low fringe number around 770 nm, that is $m = 31$, and for a higher fringe number, $m = 45$, at around 555 nm as the temperature changes different trends are seen. For short wavelengths T_{\max} decreases with temperature and at longer wavelengths T_{\max} increases. Notice that these results are reproducible since they were measured during the second high temperature heating phase so that permanent changes have stabilized. Such variations are a surprise at first sight, see figures 11(a) and 11(b) for details. Without a detailed study an appreciation of this effect can be gained by investigating the equation describing T_{\max} for a Fabry Perot showing absorption. Simple reflectivity type calculations lead to an expression of the form

$$T_{\max} = \frac{(1-R_1)(1-R_2)e^{-2ad}}{(1 - \sqrt{R_1 R_2} e^{-2ad})^2}$$

Since we know the wavelength at which the maxima occur and d , the layer thickness, we can calculate the refractive indices and thus the reflectivity at the front face, R_1 , and the back face, R_2 . Taking the experimental values for T_{\max} it is straightforward to calculate that for a fringe where $m = 45$ that $\Delta(2ad) \sim 0.01$. Thus the absorption, a , increases as the temperature increases. Conversely, repeating the procedure for a fringe with $m = 31$ calculations show that $\Delta(2ad) \sim -0.07$, so that the absorption, a , decreases with increasing temperature. This brief calculation serves to show that changes in refractive index are not responsible for the effects. Variations in the absorption characteristic is not straightforward.

Similar temperature related absorption changes are seen in the higher temperature grown samples but are less pronounced. Variations with temperature cycling for the 150°C grown sample are represented in figure 12. Shown are the spectra measured at room temperature, before heating, after raising the temperature to 225°C and cooling and then repeating the temperature cycle. Reproducible spectral variations with temperature are illustrated in figure 13. Absorption edge alterations with temperature cycling of the 300°C grown sample are shown in figure 14. Spectra are at room temperature for the as grown sample, after raising to 225°C and cooling once, and twice. A demonstration of how the spectra vary with increasing temperature is given in figure 15. As has been noted before, increasing and decreasing the temperature of the sample leads to a permanent sharpening of the absorption edge, this effect being more pronounced for the lower growth temperature sample. It is instructive to compare the final spectra at 25°C for each of the three samples after temperature cycling, see figure 16. As can be seen these final spectra are now similar. Differences that remain are the thicknesses and the refractive indices which both contribute to placing the interference maxima at different wavelengths.

CONCLUSIONS

Study of MBD grown samples of ZnSe at three substrate growth temperatures has been completed using a simple spectrometer measurement of the absorption edge and the interference fringes. Two main conclusions are, firstly, that the refractive index of the material increases with increasing temperature and exhibits reproducibility but that secondly, permanent changes in the absorption are caused by the increased temperature. Such changes are more pronounced for the lower growth temperature sample where the initial absorption is greater. From these results it can be conjectured that temperature cycling causes the defect structure to be dramatically changed, may be by microcrystallite grain growth, resulting in vast differences in transmission. Associated changes in absorption are in fact relatively small and through the Kramers-Kronig relation so too is the expected change in the refractive index. Induced changes in refractive index are too small to be detected in this type of experiment. A more abrupt absorption edge suggests a more defect free material. Such conjectures can be tested with TEM studies. This careful analysis has led to accurate values of $n(\lambda, T)$ for three growth conditions and has allowed dn/dT to be calculated over the whole of the visible spectrum.

We can see already that these optical changes can have significant effects on ZnSe optical devices. Previous studies have shown that Fabry-Perot etalons used as optically bistable switches suffer from variations in switching intensities with operation, see [1] and [9]. A Fabry-Perot operating in bistable mode is highly sensitive to small changes in n and α . Alterations in the switching powers can be reinterpreted as variations in the critical detuning of the device, that is the detuning necessary for the onset of optical bistability. From a simple theoretical treatment we have the critical detuning, δ_c , given by;

$$\delta_c = -\frac{\sqrt{2}}{4} \frac{G(F)}{H(F)} + \sin^{-1} \left\{ \left[\frac{(3F+2) - \sqrt{[(F+2)^2 + 8F^2]}}{4F} \right]^{\frac{1}{2}} \right\}$$

where

$$G(F) = 3(F+2) - \sqrt{[(F+2)^2 + 8F^2]}$$

$$H(F) = \left\{ (F+2) \sqrt{[(F+2)^2 + 8F^2]} - (F+2)^2 - 2F^2 \right\}^{\frac{1}{2}}$$

$$F = \frac{4 \sqrt{R_1 R_2} e^{-2\alpha d}}{\left(1 - \sqrt{R_1 R_2} e^{-2\alpha d} \right)^2}$$

If typical values of refractive index and absorption in ZnSe at longer wavelengths are fed into this equation it is possible to show that when $T_{\max} \sim .75$ the critical detuning is $\sim 21^\circ$ but if the absorption changes so that $T_{\max} \sim .80$ the critical detuning is dramatically altered to $\sim 32^\circ$. This is only a 7% change in transmission but it has dramatic effects. At shorter wavelength T_{\max} can alter from .2 to .3, a 50% change, and hence the change in δ_c will be even more dramatic. It is clear then that small changes in the ZnSe material can cause significant effects in δ_c and thus the switching powers in a bistable device. Thus it is expected that these effects will be more significant at shorter wavelengths. A point worth noting is that a rapid change of switching conditions is to be expected on the first operation of the device when the temperature is increased for the first time. This effect should be observable for even small temperature increases of 50°C . Since it is believed at present that the initial dramatic change in the material is proportional to temperature but that further changes occur slowly when the material is reheated to the initial temperature it is conjectured that the operating conditions of the devices should continue to alter. This is indeed observed. However, little can be said at this stage about the timescale over which this should occur. Presumably variations of material will be reduced for the high growth temperature material.

FUTURE PROGRESS

Any use of thin film ZnSe in optical applications will be susceptible to alterations in the material properties. Experiments with optically bistable devices are a sensitive method of detecting such changes but even relatively simple filter applications using ZnS can show dramatic variations in filter pass band with temperature cycling, see Roche et al [15] or Title [16]. So, imperfect ZnSe material will hinder the stability of all optical applications to which it is put. A need exists to study what causes the changes in absorption and how growth conditions can be modified to produce better material. It is already known that Zn and Se interstitials cause band gap states and hence will contribute to the broadening of the absorption edge as observed. Because the sticking coefficient of the Zn and Se₂ species during growth is temperature dependent the proportion of interstitial type defects will be expected to be dependent on growth conditions. One idea is to grow ZnSe with an over pressure of one or the other species to help keep the proportions of Zn and Se equal on the substrate thus hopefully reducing the defect density. This could lead to material showing a more abrupt absorption edge and greater stability in temperature cycling.

These tasks are planned in future work.

ACKNOWLEDGEMENTS

To Keith Lewis and Ian Muirhead for the growth of the samples at RSRE and Alan Miller for instructive discussions.

REFERENCES

- 1 S D Smith, B S Wherrett and A C Walker
All-optical limiters. MOD Contract No 2195/014/DCVD - RV RU-46-6
Final Report from Heriot-Watt University.
- 2 J Starmolynska, K L Lewis, A Miller
Optical Bistability Studies of an MBE grown/thermally evaporated ZnSe
interference filter
RSRE Memo No 3959 (Unclassified)
- 3 A Miller, I T Muirhead, K L Lewis, J Staromlynska and K Welford
Optical Bistability in MBD ZnSe/BaF₂ multilayer interference filters
J de Phys (1988) C2 6, 49, p105.
- 4 Y T Chow, B S Wherrett, E Van Stryland, B T McGuckin, D Hutchins,
J G H Mathew, A Miller and K L Lewis
CW laser pumped optical bistability in thermally deposited and molecular
beam grown ZnSe interference filters
J Opt Soc Am B (1986) 3, p1535.
- 5 A Miller, J Staromlynska, I T Muirhead, K L Lewis
Wavelength dependence of optical bistability in molecular beam deposited
ZnSe interference filters
J Mod Optics 1988 35, 3, p529.
- 6 A Miller, I T Muirhead, K L Lewis, J Staromlynska, K R Welford
Critical Switching Conditions in MBD ZnSe/BaF₂ etalons
Proc IQEC'88 Tokyo.
- 7 K L Lewis, J A Savage
A fundamental approach towards improved optical coating
Proc Boulder laser damage Symposium (1983).
- 8 K L Lewis, A M Pitt, J A Savage, A G Cullis, N G Chew, L Charlwood
The microstructure and optical properties of thin films prepared by
molecular beam techniques
Proc Topical Conference on Basic Properties of Optical Materials
(1985).
- 9 M S Hazell, M F Lewis, C L West
Investigation into the characteristics of ZnSe interference filters
RSRE Memo No 3993 (Unlimited).
- 10 C J C Thompson, A G DeBell, W L Wolfe
Refractive index of ZnSe at 3.8 μ m and 10.6 μ m, from 80 K to 300 K
Appl Optics (1979) 18, 13, p2085.
- 11 J A Wunderlich, L G DeShazer
Visible optical isolator using ZnSe
Appl Optics (1977), 16, 6, p1584.
- 12 H A S Bristow, J Hill, K L Lewis and K Hall
ZnSe Laser Windows AWRE/44/86/144.

- 13 K L Lewis, A M Pitt, J A Savage, A G Cullis, N G Chew, L Charlwood
Molecular beam techniques for optical thin film fabrication
Proc Boulder Laser Damage Symposium (1985).
- 14 J D Jackson
Classical Electrodynamics, Second Edition, Wiley, 1975, p286.
- 15 P Roche, L Bertrand and E Pelletier
Influence of temperature on the optical properties of narrow band
interference filters
Optica Acta (1976) 23, 6, p433.
- 16 A M Title
Drift in interference filters 2 : Radiation effects
Appl Optics (1974) 13, 11 p2680.

- Fig 1 Spectral response of the 300°C grown sample recorded at room temperature showing the order number of the interference fringes. An illustration of a typical spectrum.
- Fig 2 SEM micrograph of a gold coated edge of a cut ZnSe sample, the top region is the deposited film and the lower region shows the glass substrate. This particular sample is the 300°C grown sample after temperature cycling.
- Fig 3 Schematic diagram of interference maxima showing expected modification due to rapidly varying absorption and resulting wavelength shift.
- Fig 4(a) Experimental data from the 300°C grown sample, measured at room temperature, showing an attempted fit to a 2 parameter Sellmeiers equation in linear form.
- Fig 4(b) The same data and theoretical fit as in 4(a) but here represented in the more conventional format of n.v. .
- Fig 5 Theoretical fit to the experimental data taken as the temperature of the 300°C grown sample is increased for the first time using a three parameter Sellmeiers equation.
- Fig 6 Fitting coefficients for 25°C grown sample for both increasing and decreasing temperature phases demonstrating only a systematic variation with temperature and not from phase to phase.
- Fig 7 Fitting coefficients for 25°C grown sample after data set averaging, showing least squares fits.
- Fig 8 Dispersion of refractive index for the three differently grown samples all measured at room temperature, compared with the dispersion of bulk ZnSe.
- Fig 9 Rate of change of refractive index with temperature shown for the three different growth temperature samples.

- Fig 10 Transmission spectra of 25°C grown sample measured at room temperature after various temperature increases. Shown is the initial, as grown, response, 1, the spectrum after heating to 75°C then cooling back to room temperature for measurement, 2, and the spectra after two individual heatings to 225°C, 3 and 4, respectively.
- Fig 11 Variation of two interference fringes, one at short wavelength and one at long wavelength demonstrating the opposite change in T_{max} .
- Fig 12 Spectra recorded at room temperature for the sample grown at 150°C. Curve 1 corresponds to the as grown condition, Curve 2 to the modified spectrum due to heating the sample to 225°C and cooling and Curve 3 to the further modified spectrum due to a second heating to 225°C. Note the change in the absorption is significant but a change in the refractive index is not evident.
- Fig 13 Spectra recorded at elevated temperatures for the sample grown at 150°C showing the absorption and refractive index changes. These measurements are taken after the initial permanent absorption changes have occurred.
- Fig 14 Spectra recorded at room temperature for the sample grown at 300°C. Curve 1 is the as grown sample, Curve 2 after the sample has been temperature cycled to 225°C and Curve 3 after the sample has been temperature cycled to 225°C for a second time.
- Fig 15 Spectra shown the effect of temperature on the refractive index and absorption edge for the 300°C grown sample.
- Fig 16 Spectra recorded for the 3 samples at room temperature after each has been temperature cycled to 225°C twice.
- Fig 17 Spectra recorded for 3 samples at 25°C before any temperature increasing performed ie as grown.

TABLE 1

		MEASUREMENT TEMPERATURE																																
		25°C						75°C						125°C						175°C						225°C								
		A ₁	A ₂	B ₂	A ₁	A ₂	B ₂	A ₁	A ₂	B ₂	A ₁	A ₂	B ₂	A ₁	A ₂	B ₂	A ₁	A ₂	B ₂	A ₁	A ₂	B ₂	A ₁	A ₂	B ₂									
S A M	Up 1	4.155	.802	.153	4.191	.801	.155	4.310	.717	.165	4.256	.777	.162	4.274	.779	.163	P L E	300°C GROWN SAMPLE	Up 1	3.652	.720	.157	3.735	.665	.158	3.712	.700	.157	3.750	.681	.161	3.742	.704	.161
	Down 1	4.158	.806	.152	4.175	.806	.154	4.269	.750	.160	4.315	.726	.166	4.274	.779	.163			Up 2	3.679	.697	.153	3.686	.706	.154	3.770	.654	.161	3.479	.905	.144	3.742	.704	.161
	Up 2	4.158	.806	.152	4.199	.788	.155	4.211	.795	.157	4.248	.781	.161	4.316	.741	.167			Down 1	3.679	.697	.153	3.674	.717	.153	3.741	.676	.159	3.664	.753	.155	3.766	.683	.164
	Down 2	4.212	.757	.156	4.205	.782	.156	4.244	.766	.159	4.241	.790	.159	4.316	.741	.167			Up 2	3.679	.697	.153	3.704	.691	.155	3.700	.712	.156	3.705	.720	.158	3.766	.683	.164
	Up 1	3.652	.824	.146	3.801	.712	.157	3.772	.751	.156	3.837	.710	.162	3.901	.671	.168			Down 2	3.679	.697	.153	3.704	.691	.155	3.700	.712	.156	3.705	.720	.158	3.766	.683	.164
	Down 1	3.754	.737	.152	+	+	+	+	+	+	+	+	+	+	+	+			Down 2	3.679	.697	.153	3.704	.691	.155	3.700	.712	.156	3.705	.720	.158	3.766	.683	.164

+ Data not recorded

TABLE II

	25°C		75°C		125°C		175°C		225°C						
	A ₁	A ₂	B ₂	A ₁	A ₂	B ₂	A ₁	A ₂	B ₂	A ₁	A ₂	B ₂			
25°C GROWN SAMPLE	4.171	.792	.153	4.193	.7939	.155	4.260	.756	.160	4.266	.768	.162	4.296	.760	.165
150°C GROWN SAMPLE	3.711	.775	.150	3.778	.733	.155	3.786	.740	.157	3.834	.716	.162	3.906	.670	.168
300°C GROWN SAMPLE	3.670	.705	.152	3.700	.694	.155	3.732	.685	.158	3.657	.785	.155	3.755	.693	.163

+ Spurious results

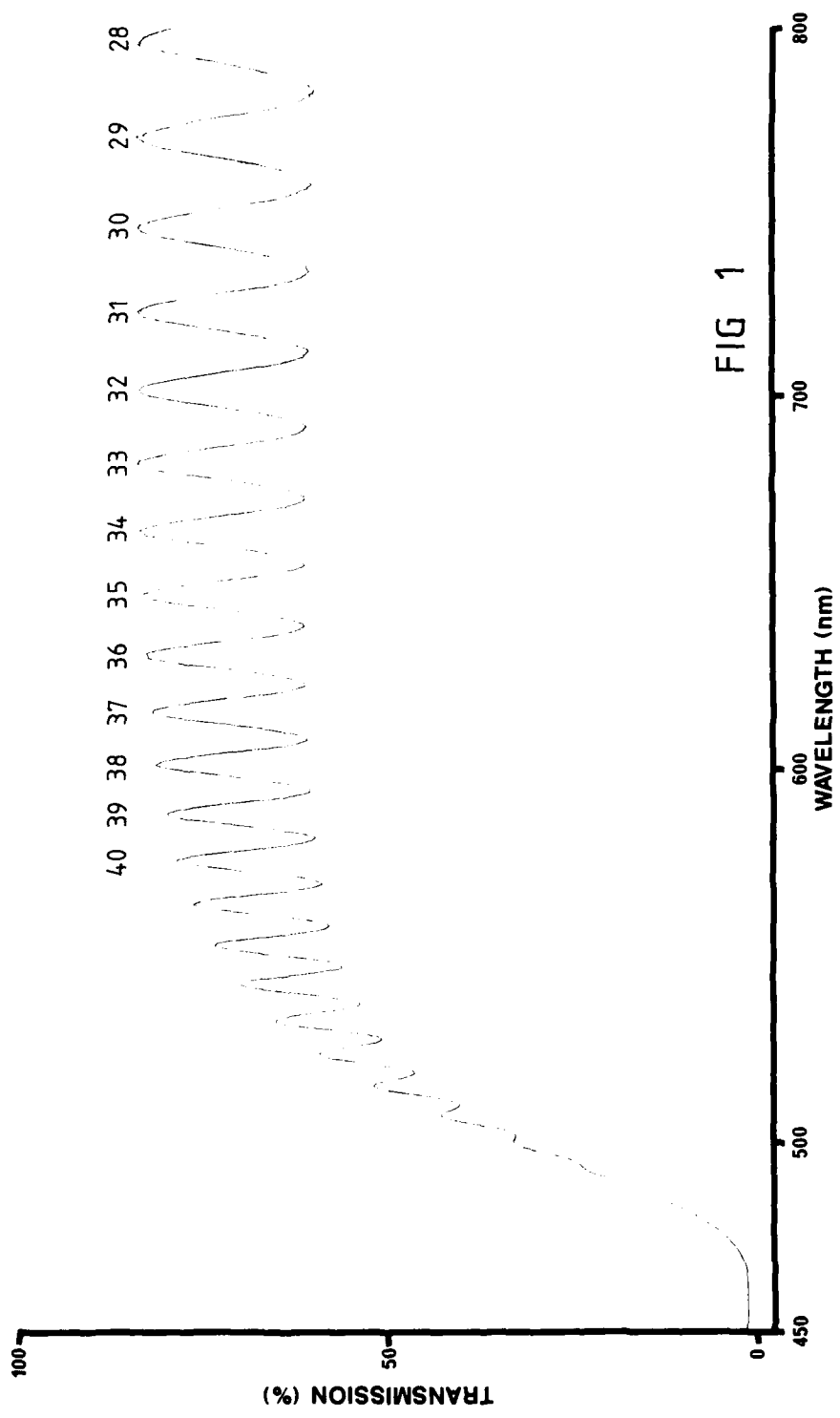


FIG 1

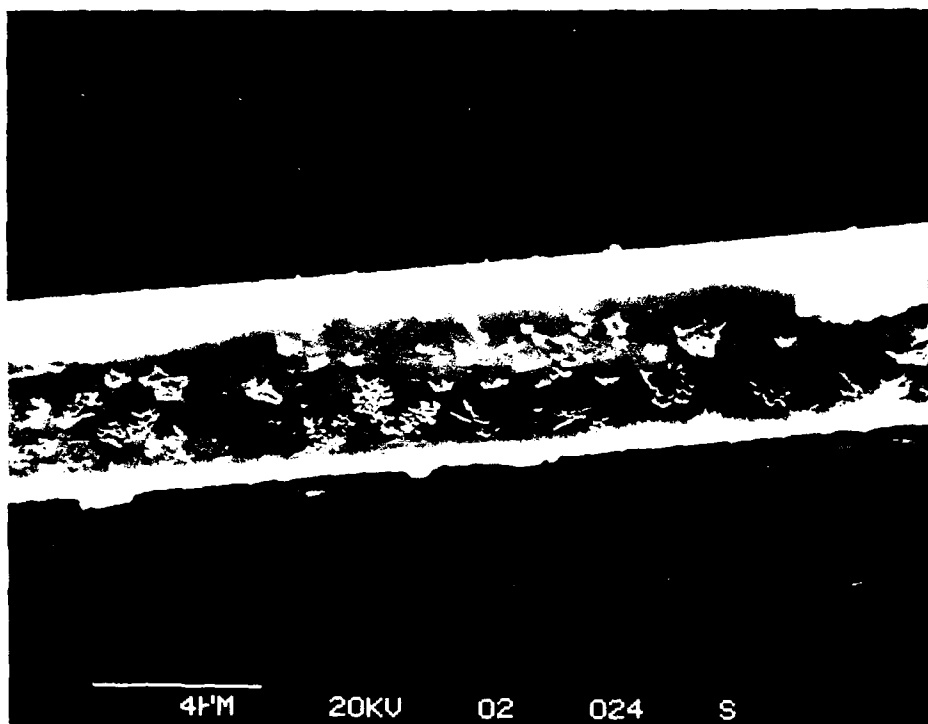


FIG 2

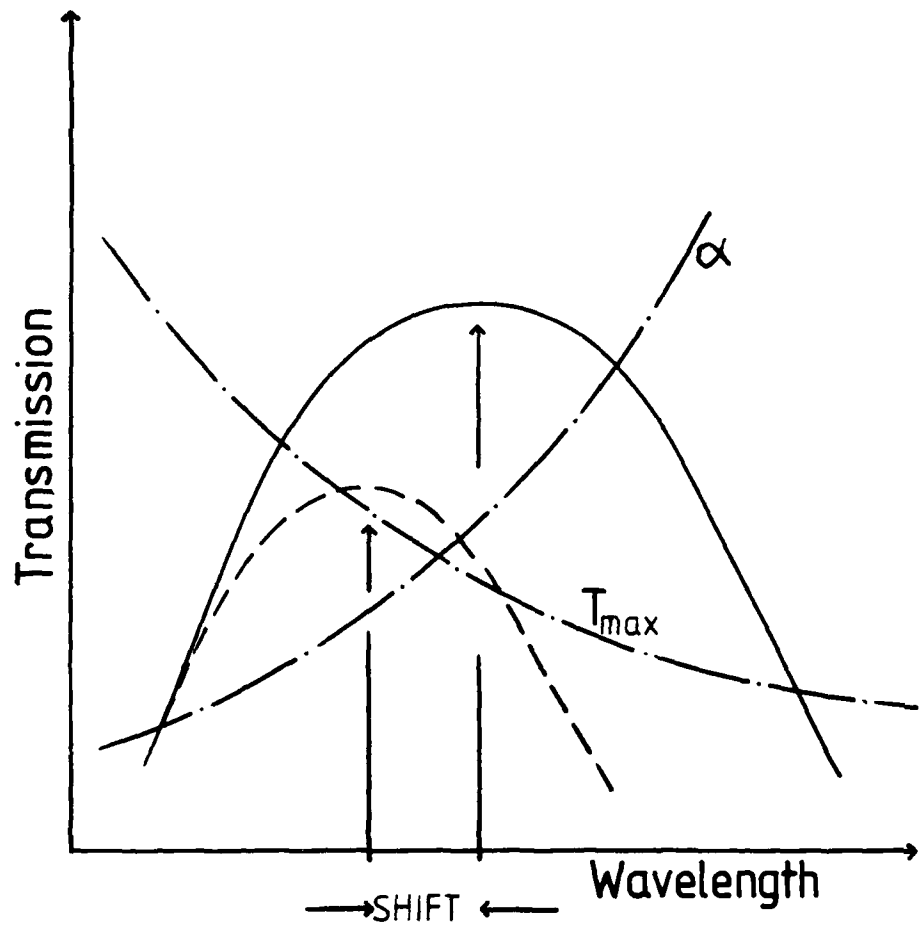


FIG 3

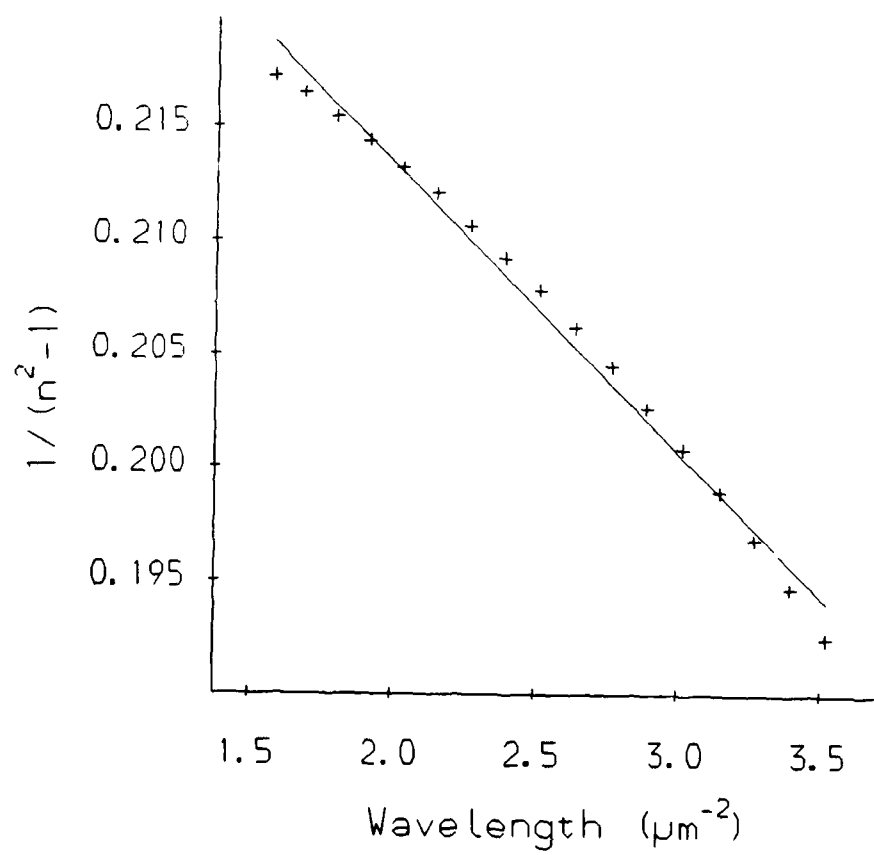


FIG 4(a)

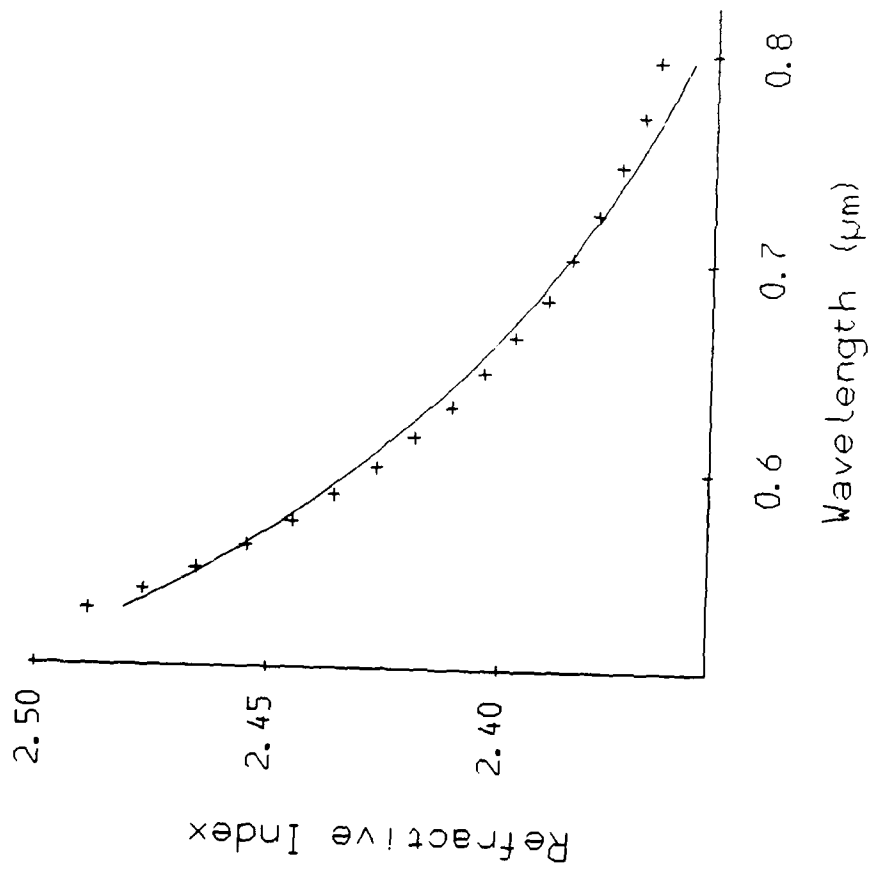


FIG 4(b)

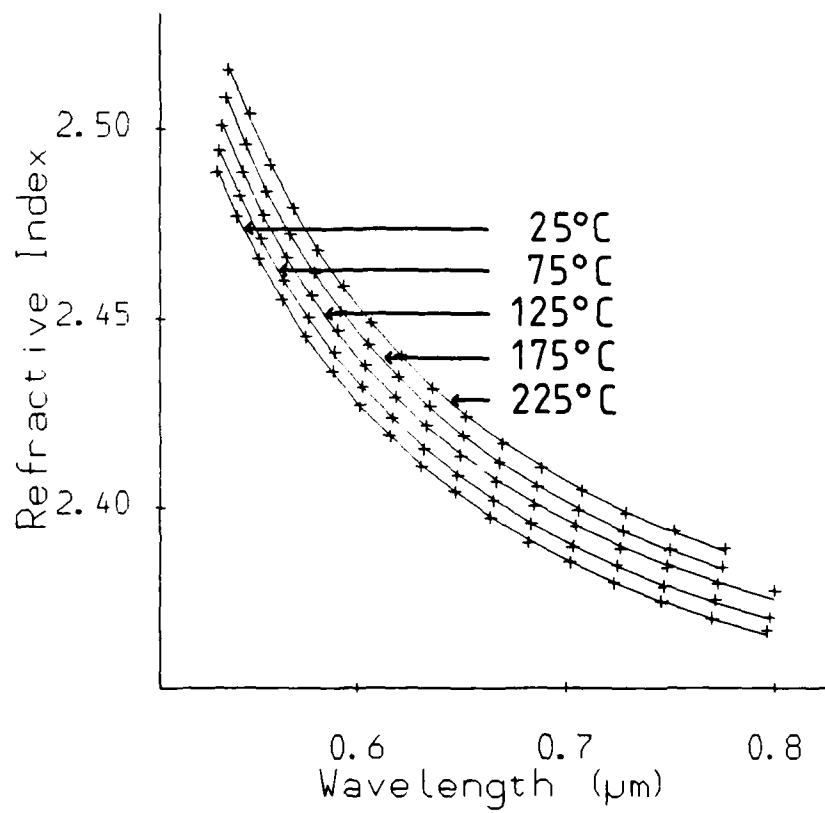


FIG 5

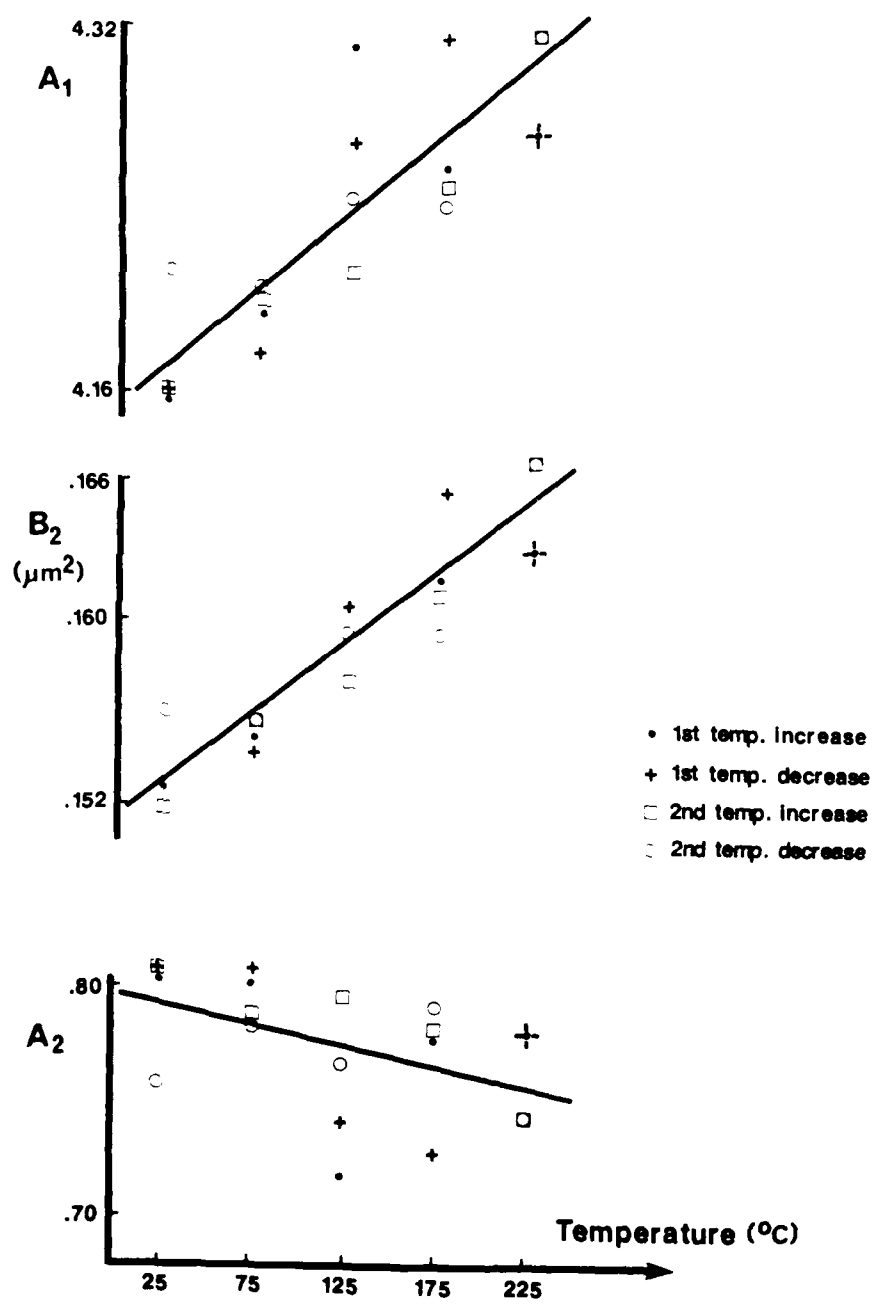


FIG 6

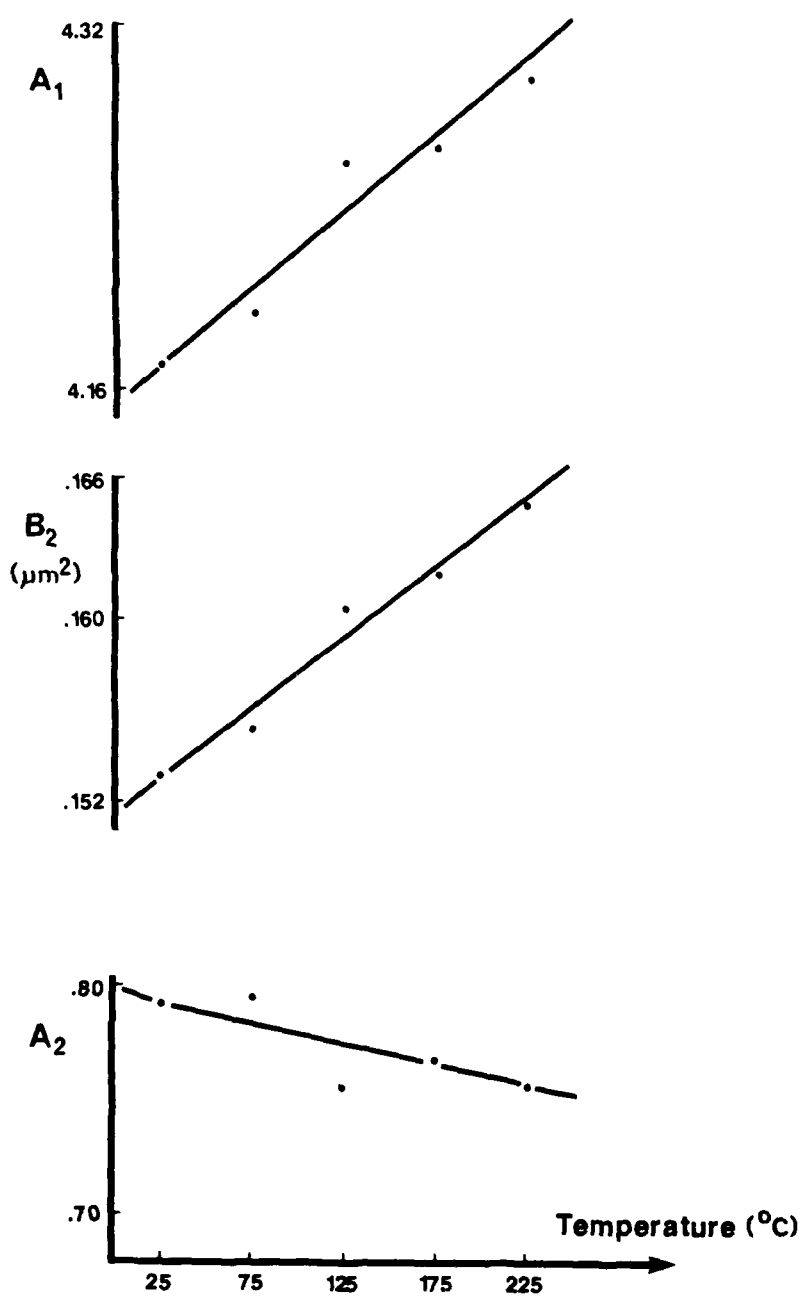


FIG 7

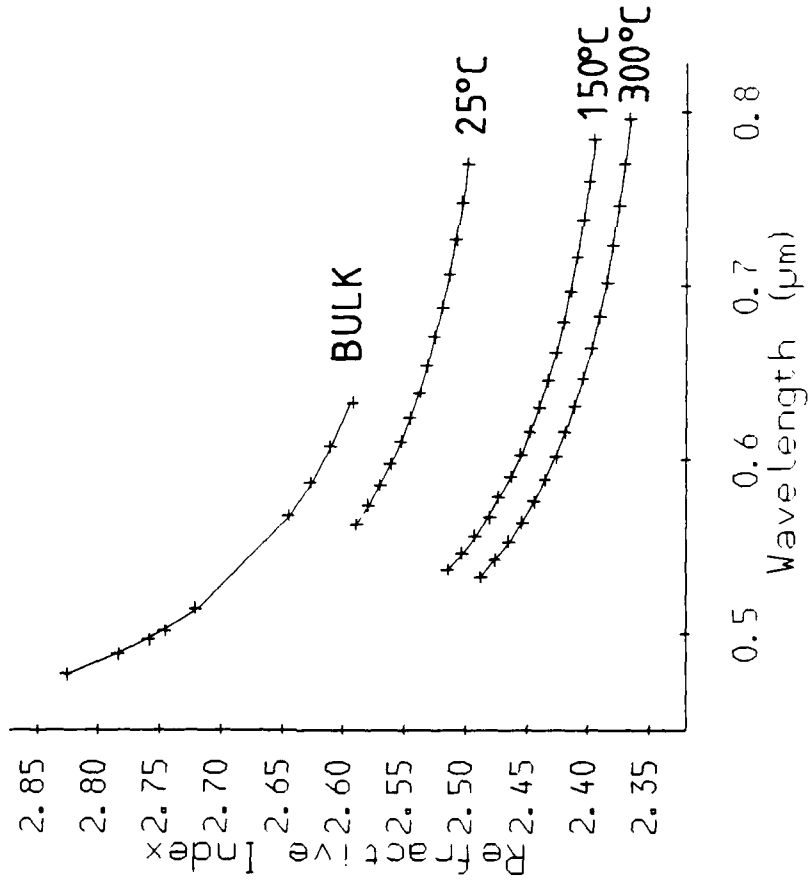


FIG 8

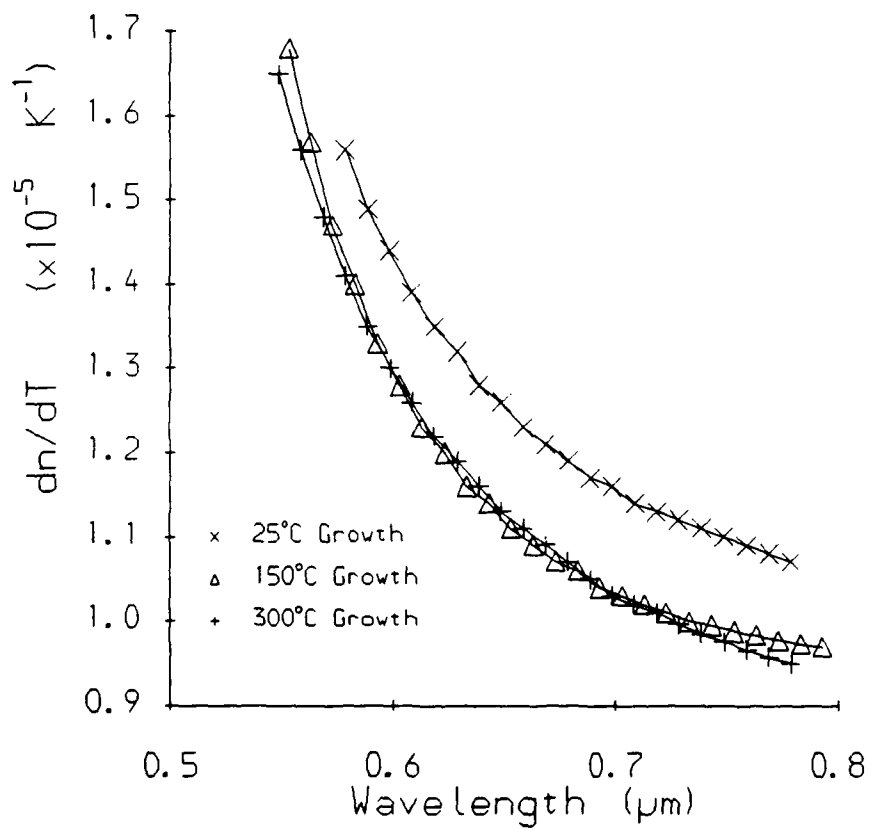


FIG 9

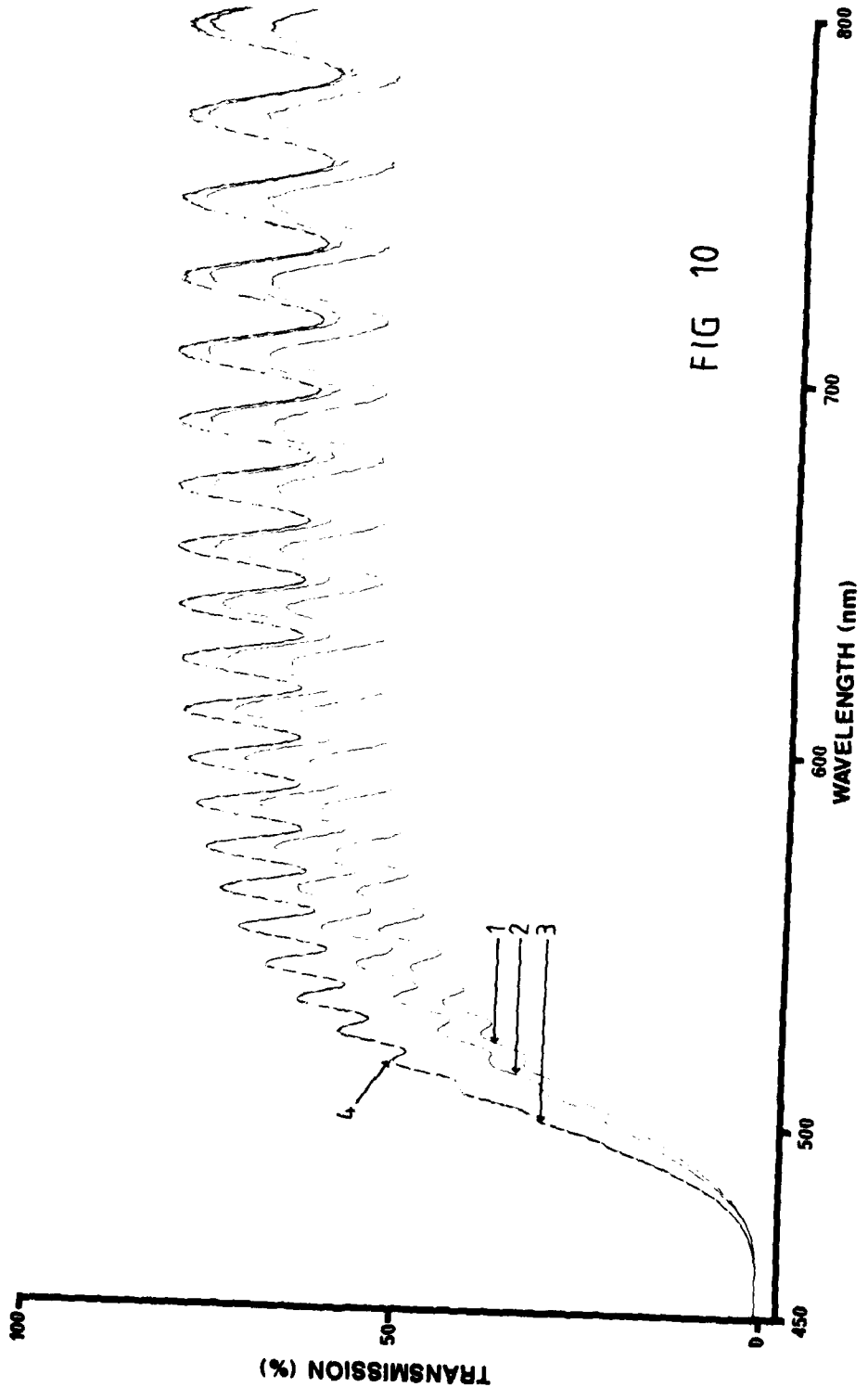
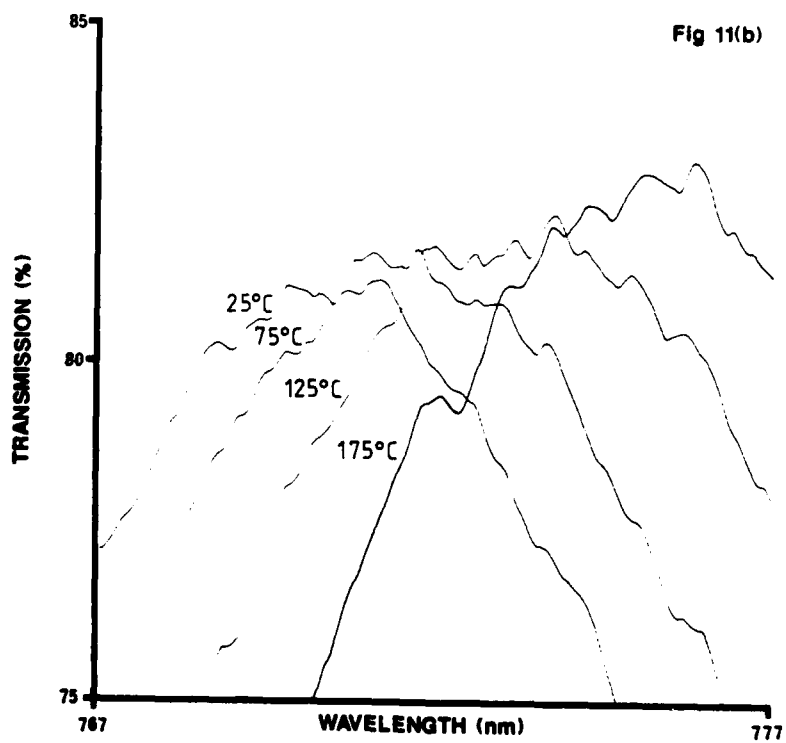
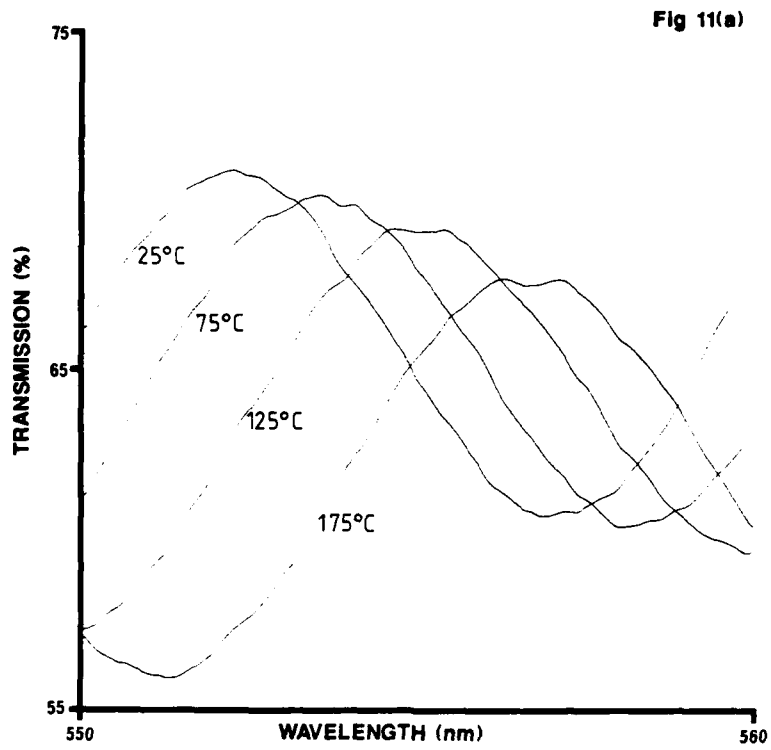


FIG 10



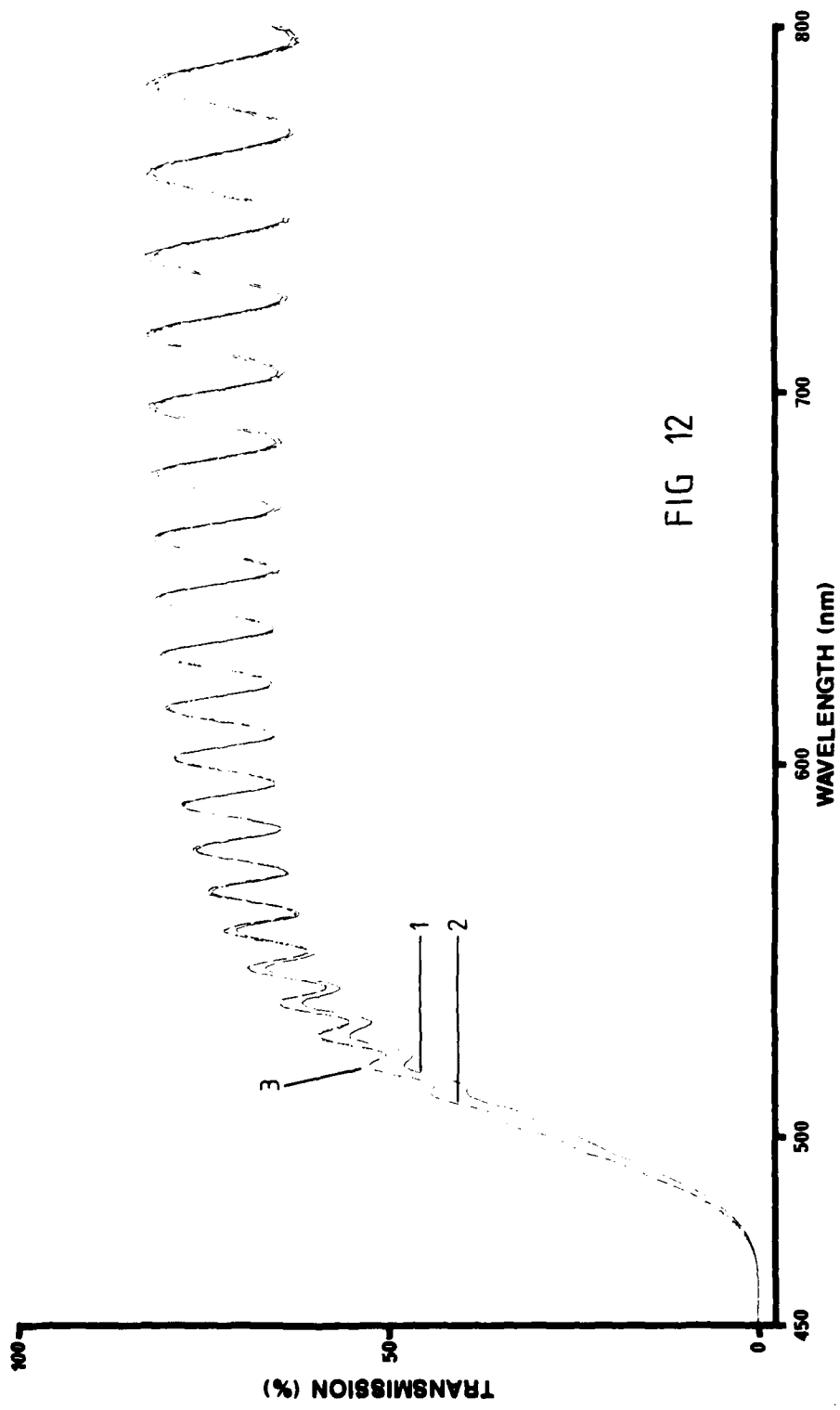


FIG 12

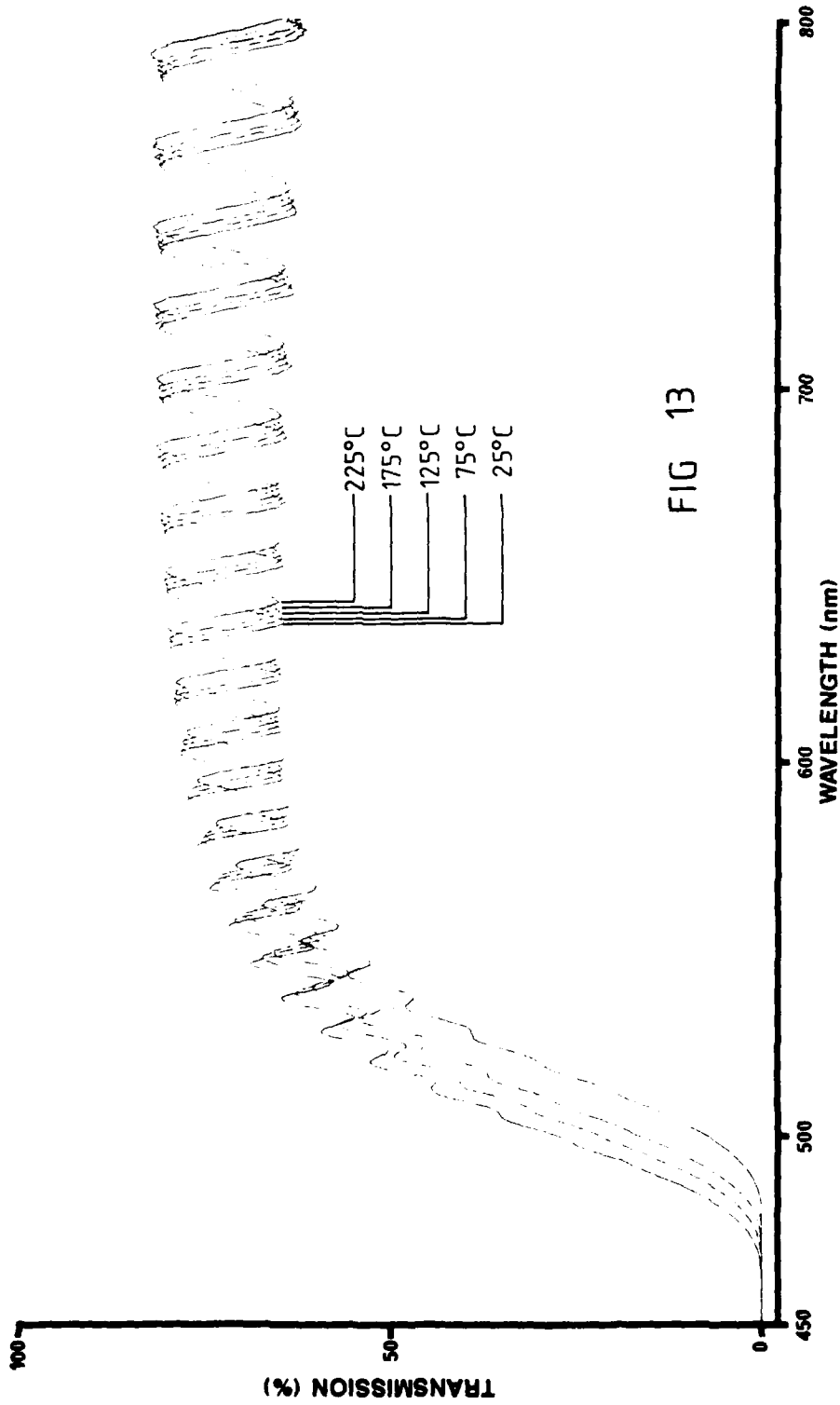


FIG 13

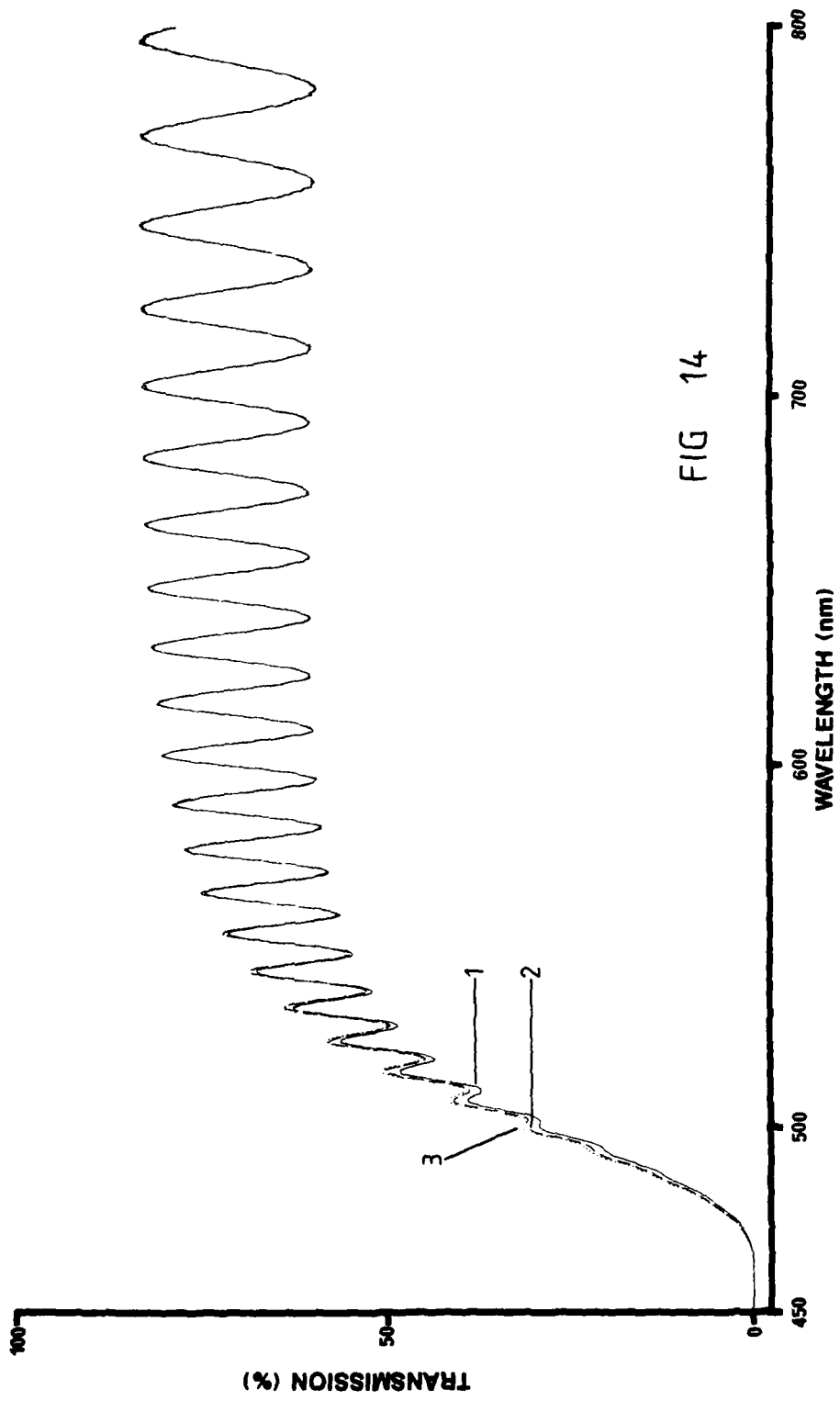


FIG 14

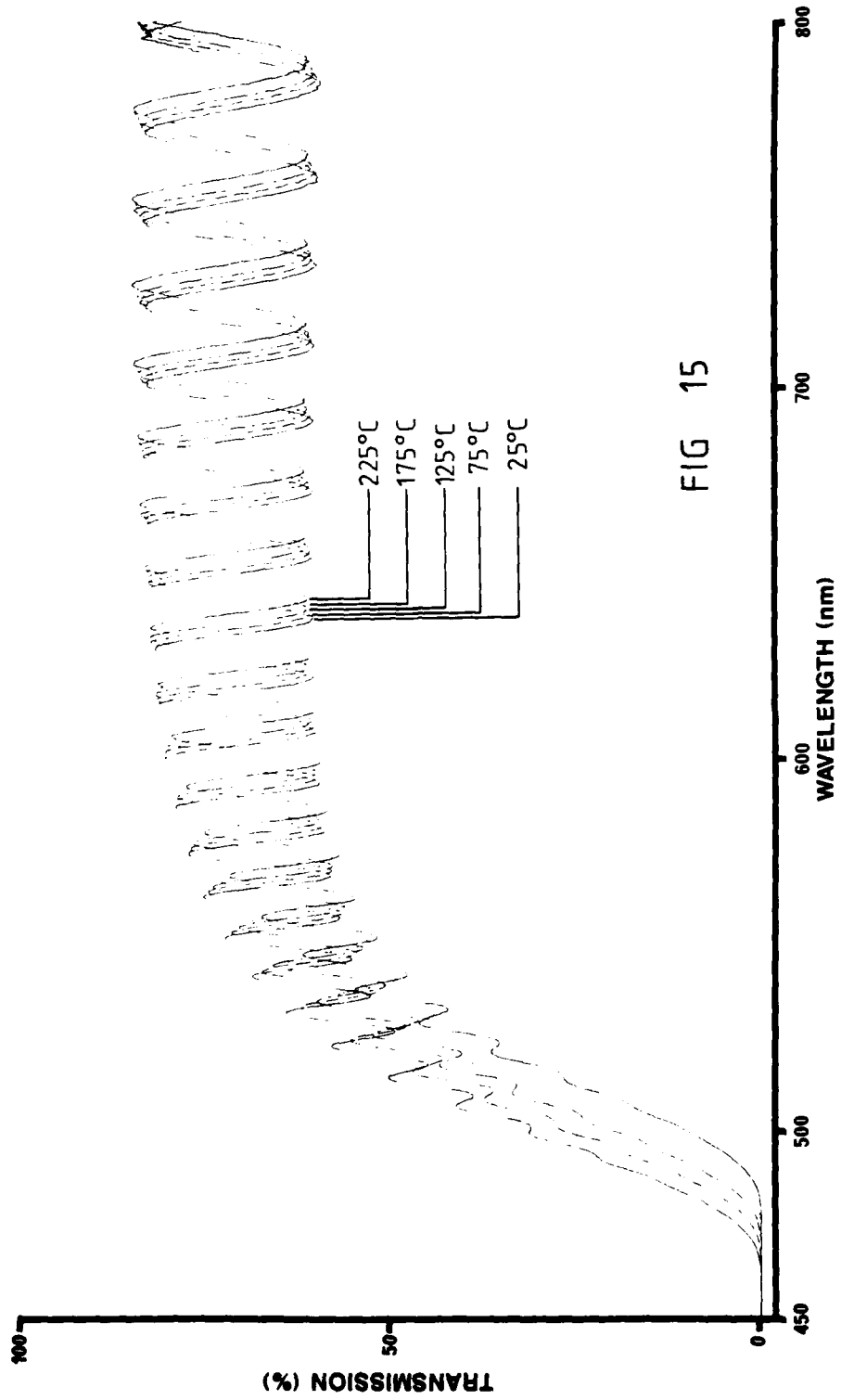


FIG 15

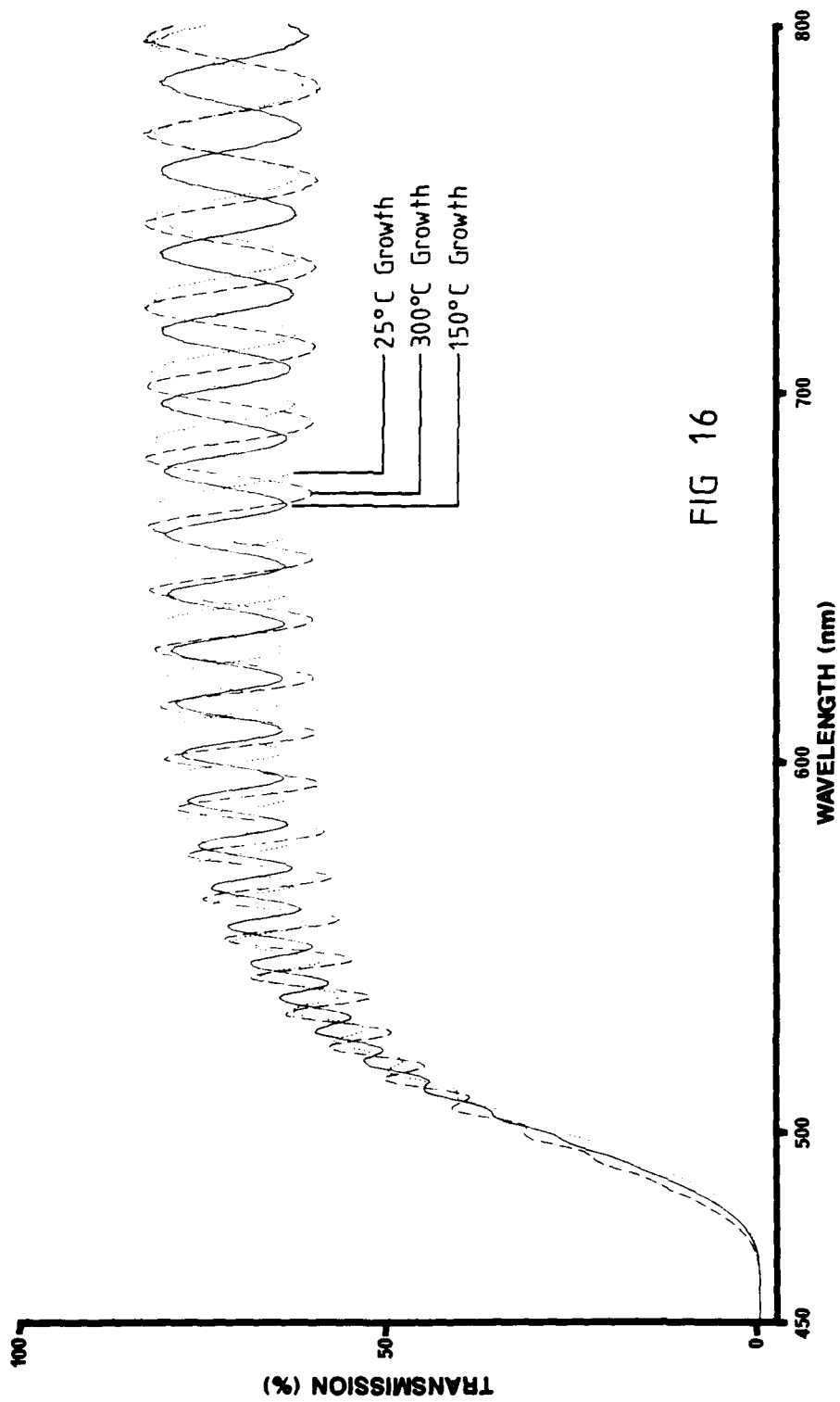


FIG 16

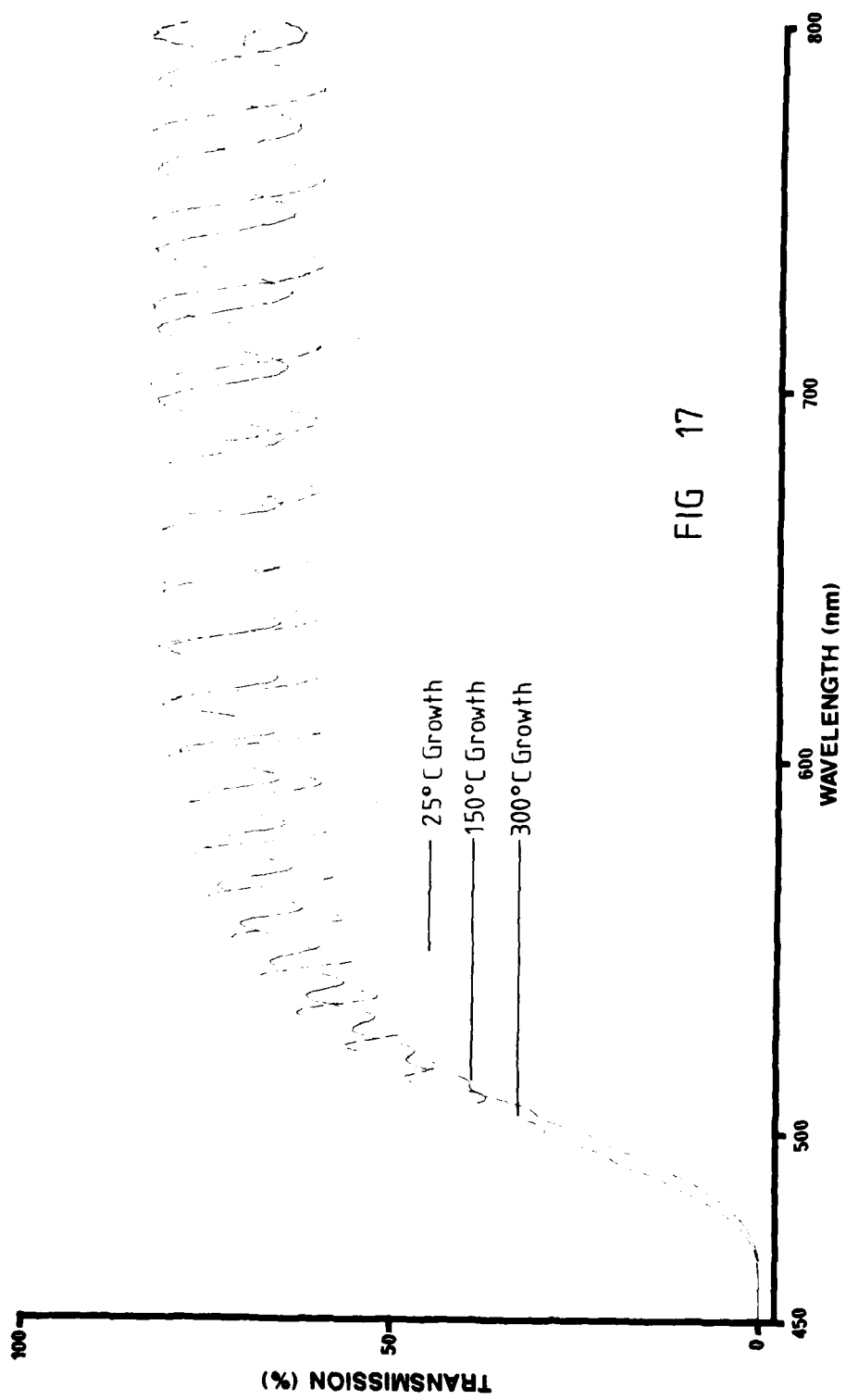


FIG 17

DOCUMENT CONTROL SHEET

Overall security classification of sheet UNCLASSIFIED

(As far as possible this sheet should contain only unclassified information. If it is necessary to enter classified information, the box concerned must be marked to indicate the classification eg (R) (U) or (S))

1. DRIC Reference (if known)	2. Originator's Reference MEMO 4269	3. Agency Reference	4. Report Security U/C Classification	
5. Originator's Code (if known) 7784000	6. Originator (Corporate Author) Name and Location ROYAL SIGNALS AND RADAR ESTABLISHMENT ST ANDREWS ROAD, GREAT MALVERN WORCESTERSHIRE WR14 3PS			
5a. Sponsoring Agency's Code (if known)	6a. Sponsoring Agency (Contract Authority) Name and Location			
7. Title OPTICAL PROPERTIES OF ZINC SELENIDE GROWN USING MOLECULAR BEAM DEPOSITION TECHNIQUES				
7a. Title in Foreign Language (in the case of translations)				
7b. Presented at (for conference papers) Title, place and date of conference				
8. Author 1 Surname, initials WELFORD K	9(a) Author 2	9(b) Authors 3,4...	10. Date 1989.06	pp. ref. 34
11. Contract Number	12. Period	13. Project	14. Other Reference	
15. Distribution statement UNLIMITED				
Descriptors (or keywords)				
continue on separate piece of paper				
Abstract For the first time the refractive index of MBD grown ZnSe films has been measured for three different growth temperatures and the wavelength and temperature dispersions quantified. Permanent absorption, but not refractive index, changes have been identified for the first time. Possible origins of the changes are conjectured along with the significant effects they will cause in optically bistable devices. Future studies are outlined which it is hoped will go some way towards producing better quality material and thus devices.				